

AD-A134 094

STUDIES OF THE ELECTRONIC PROPERTIES OF  
TWO-DIMENSIONALLY CONFINED CARRIERS. (U) UNIVERSITY OF  
SOUTHERN CALIFORNIA LOS ANGELES A MADHUKAR 17 MAY 83

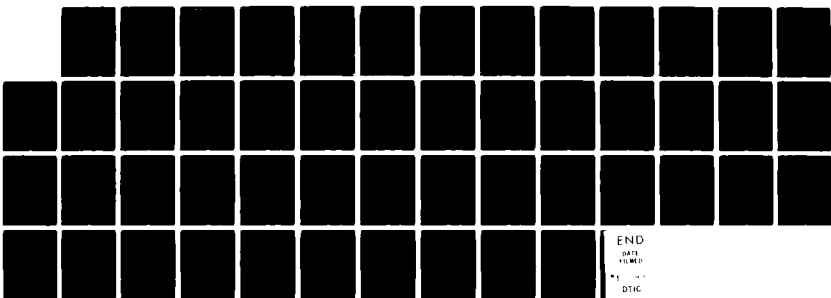
F/G 20/12

UNCLASSIFIED

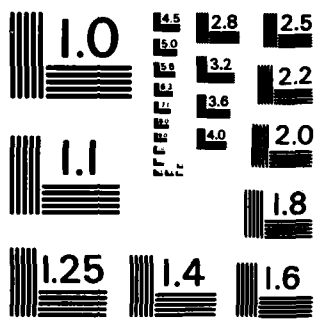
AFOSR-TR-83-0767 AFOSR-78-3530

1//

NL



END  
DATA  
112482  
\* 1  
DTIC



MICROCOPY RESOLUTION TEST CHART  
NATIONAL BUREAU OF STANDARDS - 1963 - A

SECURITY CLASSIFICATION

THIS PAGE (When Data Entered)

READ INSTRUCTIONS  
BEFORE COMPLETING FORM

REPORT DOCUMENTATION PAGE		1. REPORT NUMBER <b>AFOSR-TR- 83-0762</b>	2. GOVT ACCESSION NO. <b>AD-A134094</b>	3. RECIPIENT'S CATALOG NUMBER
4. TITLE (and Subtitle)  Studies of the Electronic Properties of Two-Dimensionally Confined Carriers in MIS Inversion/Accumulation Layers, Heterojunctions and Quantum Wells		5. TYPE OF REPORT & PERIOD COVERED Final, Dec. 1977-Mar. 31, 1983		
7. AUTHOR(s)  A. Madhukar		6. PERFORMING ORG. REPORT NUMBER <b>AFOSR-78-3530</b>		
9. PERFORMING ORGANIZATION NAME AND ADDRESS University of Southern California University Park, MC 0241 Los Angeles, CA 90089-0241		10. PROGRAM ELEMENT, PROJECT, TASK AREA & WORK UNIT NUMBERS <b>61102F 2306/131</b>		
11. CONTROLLING OFFICE NAME AND ADDRESS Air Force Office of Scientific Research (AFOSR) Bolling Air Force Base Washington, DC		12. REPORT DATE <b>May 17, 1983</b>		
14. MONITORING AGENCY NAME & ADDRESS (if different from Controlling Office)		13. NUMBER OF PAGES <b>49</b>		
16. DISTRIBUTION STATEMENT (of this Report)  Approved for public release		15. SECURITY CLASS. (of this report) <b>UNCLASSIFIED</b>		
17. DISTRIBUTION STATEMENT (of the abstract entered in Block 20, if different from Report)		15a. DECLASSIFICATION/DOWNGRADING SCHEDULE		
18. SUPPLEMENTARY NOTES				
19. KEY WORDS (Continue on reverse side if necessary and identify by block number)  Confined charge carriers, quantum wells, heterojunctions, superlattices, III-V semiconductors, low temperature carrier mobility, remote ion scattering, interface roughness scattering, alloy disorder scattering, screening effects, quantum size effect, interaction, anomalous acoustic plasmon, magnetotransport, Shubnikov-de Haas effect, screening under high magnetic field, InP accumulation layer (cont.)				
20. ABSTRACT (Continue on reverse side if necessary and identify by block number)  This is the final report on the theoretical work done during Dec. '77-Mar. '83 under grant AFOSR-78-3530. It reports the results of several investigations of the one and many electron transport, magneto-transport, optical and magneto-optical properties of quasi two-dimensionally confined charge carriers realized in metal-insulator-semiconductor (MIS) inversion or accumulation layers, heterojunctions, and multiple, isolated or coupled, quantum well structures involving III-V compound semiconductors and their alloys.				

DD FORM 1 JAN 73 1473 EDITION OF 1 NOV 68 IS OBSOLETE

83 10 04 080

SECURITY CLASSIFICATION OF THIS PAGE (When Data Entered)

UNCLASSIFIED

DMC FILE COPY

SECURITY CLASSIFICATION

**UNCLASSIFIED**

in Date Entered)

19. (cont.) electric subband structure.

**UNCLASSIFIED**

SECURITY CLASSIFICATION OF THIS PAGE (When Data Entered)

**FINAL SCIENTIFIC REPORT**

Grant Number: AFOSR-78-3530

Title: Studies of the Electronic Properties of Two Dimensionally Confined Carriers in MIS Inversion/Accumulation Layers, Heterojunctions and Quantum Wells

Period: Dec. 1, 1977-Mar. 31, 1983

Submitted by:

A. Madhukar  
Departments of Materials Science and Physics  
University of Southern California  
Los Angeles, CA 90089-0241

**ABSTRACT**

This is the final report on theoretical work supported by AFOSR Grant number 78-3530 during the period December 1977 through March 1983. It summarizes the salient features of the results accomplished over this period. However, greater detail is provided for work accomplished between February 1, 1982 and March 31, 1983 - a period for which this is the annual as well as final report. Details of the work completed during the period December 1977 through January 1982 may be found in the attached publications. ←

AIR FORCE OFFICE OF SCIENTIFIC RESEARCH (AFOSR)  
NOTICE OF TRANSMITTAL TO DTIC  
This technical report has been reviewed and is  
approved for public release 1A: AFR 100-12.  
Distribution is unlimited.  
MATTHEW J. KENNER  
Chief, Technical Information Division

Approved for public release;  
distribution unlimited.



*A*

## PREAMBLE

Investigations of the quantum transport, magneto-transport, optical and magneto-optical properties of quasi 2-dimensionally confined charge carriers [confined in quasi-two-dimensional potential wells created via formation of single or multiple interfaces between semiconducting materials] have, in the past six years, advanced at an unprecedented pace compared to their beginnings in the late sixties. A major part of this rapid expansion of research activity is caused by the coming of age of the techniques of metal-organic chemical vapour deposition (MO-CVD) and molecular beam epitaxy (MBE) which have been successful in fabricating remarkably perfect thin single and multiple interface structures of compound semiconductors (particularly the  $\text{GaAs}/\text{Al}_x\text{Ga}_{1-x}\text{As}$  system), thus moving the subject beyond the  $\text{Si}/\text{SiO}_2$  based metal-oxide-semiconductor (MOS) prototype structures as the sole means of creating 2-dimensionally confined electron gases. The driving force for this new class of materials and structures is, no doubt, the device potential of their new and novel properties in areas beyond the scope of the  $\text{Si}/\text{SiO}_2$  based technology. The work undertaken under the AFOSR grant number 78-3530 represents an attempt to foresee certain important and interesting aspects of the new and novel structures and to contribute to the growth of knowledge of their remarkable properties. The final report which follows, accordingly, is arranged so as to bring out (1) the sense of a coherent view which motivated a systematic approach to investigations of some of the key one and many electron properties; (2) the emphasis on the relevance of the theories developed to the real nature of the material systems and their growth and; (3) the chronological choice of the issues tackled over the period of the grant and their relationship to the evolution of the material systems themselves.

### I. THE ELECTRON-PHONON COUPLING

The primary focus of the research activity sponsored by this grant was, from its inception, the III-V compound semiconducting materials. Accordingly

one of the very first areas we tackled was the role of electron-phonon coupling in influencing the single particle and collective behaviour of quasi-two-dimensional electron gas. Prior to the studies undertaken by us it was commonly held that phonons were inconsequential to these properties at low temperatures - the oft heard argument being that the Debye frequency of the materials involved was too high compared to the relevant temperatures. The obvious fallacy of this contention, surprisingly, took an unduly long period of several years to be recognized and it is only in the past couple of years that serious attempts to investigate such issues have been undertaken by several groups around the globe. Indeed, today it seems to be an area of single particle property attracting major interest. Undoubtedly a major part in creating this situation was played by the preoccupation of the relevant research community with the inversion layer in the Si/SiO<sub>2</sub> system as well as the prejudice this experience generated. During the period Dec. '77 through Dec. '79 we provided several results indicating the importance of the electron-phonon coupling. We were, however, forced to compare the theory with the results on the Si/SiO<sub>2</sub> system since no reliable experimental results on III-V compound semiconductors existed at the time. Indeed, even many of the results on the Si-inversion layers which were well accepted at the time and provided the motivation and basis for many other theories which gained notoriety, have either been called into question or discredited by further improvements in sample preparation and increased understanding of this material system. The three major and new results we predicted on the role of the electron-phonon interaction have now borne the test of experiment and time. These are,

#### (I.1) Cyclotron Resonance Line Width

We showed that the simultaneous observation of a  $\sqrt{H}$  dependence on the magnetic field strength and linear dependence on the temperature (4°K < T < 25°K) of the cyclotron resonance line width in Si-inversion layers is a consequence of the interactive role of the scattering due to short ranged

ionized impurity potential and the acoustic phonons. (See publication number 1.)

#### (I.2) Cyclotron Resonance Mass

We gave the first full expression for the dependence of the cyclotron resonance mass on the electron density, the applied magnetic field and the temperature. The predicted behaviour showed two central features for the first time. (a) The cyclotron mass depends upon the Landau level filling factor which involves the ratio of the electron density and the magnetic field, rather than these individually. (b) The cyclotron mass increases with temperature linearly in the regime  $T > \omega_0$ , where  $\omega_0$  is a characteristic phonon frequency. For acoustic phonons,  $\omega_0$  corresponds to phonons with  $q = (\sqrt{2}/l_0)$  where  $l_0$  is the cyclotron orbit radius. In Si-inversion layers at a typical magnetic field strength of 5 Tesla,  $l_0 \approx 100\text{ \AA}$  so that  $\omega_0 \approx 2-5\text{ K}$ , thus explaining the observed temperature dependent shift of the cyclotron mass.

#### (I.3) Magneto-Optical Anomaly

Certain novel features and enhanced nature of the magneto-optical anomaly in quasi-2-dimensionally confined carriers arising due to the electron (or hole) - optical phonon coupling in quantum well structures of III-V compound semiconductors, such as the GaSb/InAs and GaAs/Al<sub>x</sub>Gal-xAs systems, were predicted. This has, in the past two years, been confirmed<sup>1,2</sup> in experiments on the GaSb/InAs heterojunctions and recently, in inversion layers in InSb. (See publication numbers 2, 4 and 5.)

#### (I.4) Shubnikov-de Haas Effect (The magneto-transconductance)

The first correct theory of the transmagneto-conductance ( $\sigma_{xx}$ ) at high magnetic fields for a system of 2-dimensionally confined electrons subject to the simultaneous influence of impurity and acoustic-phonon scattering was

developed. The contributions of these individual scattering mechanisms, of most relevance to III-V compound semiconductors, to the electron scattering time and the effective mass were clearly identified for the first time. In particular it was demonstrated for the first time that  $\tau_{xx}$  involves two different effective masses and scattering times, of which one is the scattering time in the absence of the magnetic field. It was also shown that the Landau level width appears in  $\tau_{xx}$ , thus providing an experimental way of determining the same from a study of the background conductivity. (See publication number 8.)

## II. THE ELECTRON-ELECTRON INTERACTION

The role of electron-electron interaction in the 2-dimensionally confined electron gas occurring in Si-inversion layers has been shown to be of significance for the electric subband structure. Its role in the transport properties however is not as clear, although early reports of the observed dependence of the effective mass on the electron density created a flurry of theoretical activity. In III-V compound semiconductors the role of the  $e^- - e^-$  interaction in determining single particle properties is held to be of far less significance. However, collective properties of the electron gas are crucially dependent upon this interaction. We therefore undertook an investigation of some of these aspects, a brief summary of which is provided below.

### (II.1) Plasmon Modes in Inhomogeneous Electron Gas

We investigated the possible plasmon modes in a two-component, two dimensional plasma such as may be created in the double quantum well structures of  $\text{GaAs}/\text{Al}_x\text{Ga}_{1-x}\text{As}$ , or even a single heterojunction of  $\text{InAs}/\text{GaSb}$  which involves spatially separated electrons and holes. It was shown that in addition to the regular optical and acoustic plasmon mode, a high frequency mode can exist in such a system, provided the spatial separation between the

two charge carrier components exceeds a critical length. This mode is undamped in leading order and its dispersion is linear in the wave vector in the long wave length limit. It is thus acoustic in nature, but not the same as the normal acoustic plasmon. We have referred to this mode as an Anomalous Acoustic Plasmon. The prediction (see publication numbers 3 and 7) of the existence of such a mode and its nature has recently been confirmed<sup>3</sup> in light scattering experiments conducted by Olego et al.

#### (II.2) Screening in the Presence of a Strong Magnetic Field

In the presence of a magnetic field, the constant density of states of a 2-D electron gas changes into a series of  $\delta$ -functions separated by the cyclotron energy ( $h\omega_c$ ), provided there are no broadening mechanisms. In real systems, of course, there are always scattering mechanisms, particularly the electron-impurity scattering. The screening of the impurity potential depends upon the nature of the density of states, but the density of states (i.e. broadening of the ideal  $\delta$ -functions) in turn depends upon the screened electron-impurity interaction. A meaningful understanding of the screening behaviour in the presence of a magnetic field, consequently, requires a self-consistent treatment of the problem. Such a calculation was carried out within the random phase approximation (RPA) and explicit results for the zero temperature dielectric function in the extreme quantum limit (i.e. Fermi energy in the first Landau level) were obtained. We showed that this first principles, one electron, theory of the cyclotron resonance line width was consistent with anomalous behaviour was speculated by the experimenters, and others, to be indicative of the formation of a charge density wave or occurrence of the long predicted Wigner crystal state. (See publication number 6.)

#### (II.3) Quantum Wigner Crystal

The freezing of an electron gas into a solid at low densities and ultra low temperatures was predicted by Wigner in 1932. In a two dimensional system

with an applied magnetic field, the spatial motion of the electrons is completely quantized and the possibility of realizing the quantum Wigner crystal at low densities, high magnetic field and ultra low temperatures is greatly enhanced. The anomalous observed behaviour of the cyclotron resonance line width in Si-inversion layers and  $\text{GaAs}/\text{Al}_x\text{Ga}_{1-x}\text{As}$  heterojunction, as noted in the previous section, was speculated to be a manifestation of this state or at least the formation of a precursor charge density wave. While the past five years have seen considerable theoretical work on the solid-liquid phase transition involved (i.e. theory of melting in two dimensional systems), we addressed ourselves to a somewhat more pragmatic issue - what is the signature of the existence of the quantum Wigner state in a particular non-destructive experiment which is feasible given the particular configuration (heterojunction or quantum well) of the sample? Since magneto-absorption is one such experiment, we undertook a calculation of this property for a quantum Wigner crystal as a function of the electron density, the applied magnetic field and temperature. The existence of the Wigner crystal is thus assumed as the ground state and enters the calculation of the absorption behaviour via a lattice expansion of the density-density correlation function in terms of the normal modes of the Wigner solid. These are the magneto-plasmon and acoustic phonon modes of the Wigner solid. Coupling with the acoustic phonon modes of the substrate material (i.e. material containing the electron gas), which act as the heat bath, is included, thus allowing the influence of temperature on the "softening" of the Wigner solid. The lattice absorption characteristics of such a solid were calculated for single phonon absorption as well as multiphonon processes. The predicted temperature dependence due to both these processes is  $\exp(-T_0/T)$ , where  $T_0$  is a characteristic temperature but different for the two processes. This temperature dependence is distinctly different from the linear temperature dependence of the free electron gas. Similarly, the electron density and magnetic field dependence, though quite involved, are distinctly different from that of the free electron gas. To the best of our knowledge, these results remain the only prediction of at least

one property of the quantum Wigner crystal that may make its detection feasible. (See publication number 10.)

#### (II.4) Magnetotransport in the Presence of $e^-$ -Impurity, $e^-$ -Phonon and $e^-e^-$ Interactions

In section (I.4) we reported the results for magneto-transconductance ( $\sigma_{xx}$ ) in a system subject to electron-impurity and electron-acoustic phonon interactions. The role of  $e^-e^-$  in determining the behaviour of  $\sigma_{xx}$  has long been a matter of speculation. The problem of calculating  $\sigma_{xx}$  when all three interactions are simultaneously present is a rather involved one, particularly because any correct theoretical treatment must naturally reproduce the correct results for individual scattering agencies in the appropriate limits. Such a theory must also be consistent with certain basic results of the Fermi liquid theory and must correspond to Kohn's theorem.

We undertook the development of such a theory. Via a combination of the memory function technique and spectral representation of the one electron Green's function for an electron gas with  $e^-e^-$  interactions we were successful in obtaining the first and only expression for  $\sigma_{xx}$  valid under the simultaneous influence of  $e^-$ -impurity,  $e^-$ -acoustic phonon and  $e^-e^-$  interactions. This result clearly identifies the different scattering times and effective masses occurring in  $\sigma_{xx}$ , as well as the specific contributions of the individual scattering interactions to these masses and scattering time. It thus provides a meaningful expression for analysis of reliable experimental data. (See publication number 9.)

### III. ELECTRIC SUB-BAND STRUCTURE OF InP ACCUMULATION

Interest in n-channel inversion or accumulation layers in InP arises from the high mobility afforded by the low electron effective mass ( $0.08 m_e$ ), of use in high-bit rate optoelectronic and microwave circuits. such space charge

layers in InP have been realized in the conventional Metal-Insulator-Semiconductor (MIS) structures with  $\text{SiO}_2$  and lacquer as the insulator for test purposes only. While the search for better insulators and the recent interest in forming hetero-junction and quantum wells continues, we undertook a study of the electronic subband structure of accumulation layers in MIS structures which is equally applicable to the heterojunctions. The subband energy levels and their occupancy was calculated within the Hartree-Self-Consistent scheme as a function of the electron density and temperature. It was shown that even at low temperatures ( $\sim 10^0 \text{K}$ ) and densities ( $\sim 10^{12}/\text{cm}^2$ ), the first excited electric subband is also occupied by 10% of the electrons. The presence of carriers in two subbands makes the system less 2-dimensional compared to the situation in the Si- $\text{SiO}_2$  inversion layers. These theoretical results explain the observed anomalous Shubnikov-deHaas oscillations reported for InP. (See publication number 11.)

#### IV. CARRIER MOBILITY IN QUANTUM WELL STRUCTURES

Enhancement of the carrier (generally electron) mobility over the bulk values has been demonstrated in both single and multiple interface systems by exploiting the notion of modulation doping. A variety of high speed devices such as the high electron mobility transistor (HEMT), rely upon such mobility enhancement. While considerably high electron mobilities have been achieved in the  $\text{GaAs}/\text{Al}_x\text{Ga}_{1-x}\text{As}$  system--the latest reported values reaching approximately  $2 \times 10^6 \text{ cm}^2/\text{V-sec.}$  at  $4.2^0 \text{K}$ --an understanding of the dependence of the mobility on the various factors influencing it remains an essentially open subject. Such factors may be viewed as belonging to three broad and inter-related categories--(A) The structural and chemical nature of the interfacial regionn (B) The potential experienced by the confined carriers due to the variety of doping schemes employed and (C) The self-consistent screening of all the relevant potentials causing scattering of the carriers. Given a clear and physically meaningful understanding of these three

ingredients, one may proceed with the development of an appropriate theoretical formulation and investigate the behavior of the mobility systematically as a function of doping schemes, temperature, etc. While several isolated attempts have been reported in the literature, they invariably restrict the efforts to the simplest level of both theoretical calculation and physical modelling of the material system and the relevant scattering mechanisms. It is thus not surprising that little success has been achieved in understanding the behavior of the mobility. Given such a situation we undertook a systematic investigation of a range of basic issues which need to be clearly exposed, formulated and examined to achieve a meaningful understanding of the phenomenon of mobility enhancement. In the following we provide a brief description of these investigations. Details of some of these are contained in the preprints attached herewith and others at various stages of preparation.

(IV.1) REMOTE-ION SCATTERING:

All, except one, of the previous calculations of the remote donor-ion scattering to the confined electron mobility have employed a dielectric screening function corresponding to purely 2-D electrons. The exception is the calculation<sup>4</sup> carried out by Price employing improved dielectric function which includes certain effects of the finite thickness of the electron gas layer and is given by,

$$\epsilon(q) = \left\{ 1 + \frac{S}{q} \cdot \iint dz_1 dz_2 f(z_1) f(z_2) e^{-q|z_1 - z_2|} \right\} = \left( 1 + \frac{S}{q} h(q) \right)$$

(1) where  $f(z) = |\eta_0(z)|^2$ ,  $\eta(z)$  being the envelope of the electron wave function in the confinement direction. The screening constant is given by S. The function  $h(q)$  embodies the finite thickness of the electron gas and has been omitted (i.e.  $h(q) = 1$ ) in previous calculations. We have employed equation (1) in the present calculations.

Another issue of concern is the usage<sup>4-6</sup> of the simple Fermi's Golden rule (for estimation of the scattering time) and/or Boltzmann's equation for calculation of the mobility. To avoid the inherent limitations and inadequacies of these approaches (employed even by Price) we have used the Kubo formula based memory-function technique which inherently incorporates certain self-energy and vertex corrections not present in the other approaches noted above.

Results for the remote ion-scattering contribution to the low temperature mobility were obtained for  $\text{GaAs}/\text{Al}_x\text{Ga}_{1-x}\text{As}$  single quantum well as a function of the well thickness, alloy composition, and areal electron density for both uniform and modulation doping cases. The effect of a spacer layer in the latter doping scheme has been investigated along with the quantum size effect. (See publication numbers 13 and 15.)

#### IV.2 INTERFACE 'ROUGHNESS' SCATTERING:

In structures involving modulation doping and spacer layers, the low temperature mobility acquires significant contributions from scattering due to potential fluctuations arising from the departure of the interface from ideal structural and chemical behavior. This is referred to as interface roughness scattering. Previous considerations<sup>5</sup> have restricted themselves to only structural fluctuation and that too on the basis of a model (and its parameters) which arose in the context of the inversion layer at the Si-SiO<sub>2</sub> interface. No studies have been conducted to investigate the role of chemical intermixing at the interface which, even in the best of heterostructures, is more likely to result from the growth process. We have investigated both these effects and the findings are summarized below.

##### IV.2.A STRUCTURAL FLUCTUATIONS AT THE INTERFACE:

Fluctuations in the interface away from an ideal planar geometry (but

without chemical intermixing) may be represented by the form,

$$\langle \Delta(\vec{r}_{||}) \rangle = 0, \quad \langle \Delta(\vec{r}_{||}) \Delta(\vec{r}'_{||}) \rangle = \Delta^2 \exp\{-|\vec{r}_{||} - \vec{r}'_{||}|^2/\lambda^2\}$$

where  $\Delta(\vec{r}_{||})$  is the departure from ideal plane at  $\vec{r}_{||}$ . The corresponding potential fluctuation at the interface is then taken to be

$$V(\vec{r}_{||}, z) = V_0 [\Delta(\vec{r}_{||}) \delta(z-a) + \Delta(\vec{r}_{||}) \delta(z+a)]$$

where  $V_0$  is the band edge discontinuity. As noted above, this model originated in the context of the Si-SiO<sub>2</sub> interface and has subsequently been applied to the GaAs/Al<sub>x</sub>Gal-xAs system. It represents fluctuations in the band edge discontinuity as a function of  $\vec{r}_{||}$ , (the coordinate along the interface) but is a constant in the normal direction--hence representing structural fluctuations as schematically shown below

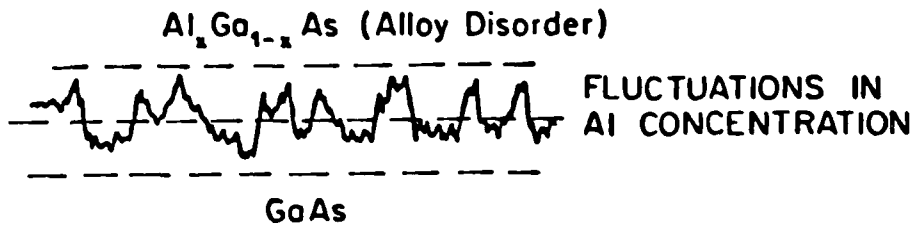


Previous calculations employing this model, and the physical picture embodied by it, have been carried out employing the Boltzman transport equation. Since the validity of the Boltzman equation in an inhomogenous electron gas, such as found at the interface is, *a priori*, not established, we carried out calculations employing this model but via the memory function technique which does not suffer from the limitations of the Boltzman equation, and provides a comparison with the previous results. We find that given all other conditions the same, the Boltzman equation overestimates the electron mobility by about 20-30%. (See publication number 15.)

#### (IV.2.B) INTERFACE ROUGHNESS DUE TO CHEMICAL DISORDER:

In structures involving III-V compound semiconductors and their alloys, there is considerable evidence of chemical disorder at and near the interface resulting during growth. Even the best grown structures indicate that this type of interface roughness exists on an atomic scale. It may thus be argued

that an alloy disorder type of roughness at and near the interface can have significant contribution to the low temperature mobility and would become the limiting factor in modulation doped structures with space layers sufficiently thick to minimize the remote ion scattering. Indeed, the barrier layer in most cases consists of a ternary alloy (e.g. in the most extensively investigated GaAs/Al<sub>x</sub>Gal-xAs system) and the penetration of the quasi-two-dimensionally confined carrier wave function into the alloy barrier layer, particularly for this quantum well, can lead to appreciable effect of the alloy disorder scattering. We have provided a model for such alloy disorder scattering at the interface and calculated its contribution to the low temperature mobility. These, the first such calculations, show that the contribution of the alloy disorder scattering at and near the interface is at least as significant as the structural imperfection model noted previously under section (B.1). (See publication numbers 14 and 15.)



#### (IV.3) ALLOY DISORDER SCATTERING IN CONFINED STRUCTURES:

A variety of single and multiple interface structures of significance involve a ternary alloy of III-V compound semiconductor as the active region of the device. Examples are the  $\text{In}_x\text{Ga}_{1-x}\text{As}/\text{InP}$  heterojunctions, the  $\text{In}_{1-x}\text{Ga}_{1-x}\text{As}/\text{Al}_y\text{In}_{1-y}\text{As}$  multiple quantum wells, etc. Since the charge carriers in such systems are confined within a thin alloy region, the alloy disorder scattering is an integral part of the transport and optical behavior of the carriers and can be expected to be the limiting factor even if remote ion scattering were minimal due to modulation doping and spacer layers. We have recently completed the very first theoretical calculations of the alloy disorder scattering contribution to the electron mobility as a function of the

thickness of the confining well, the alloy composition and carrier density. The results show significant differences from the behavior of alloy disorder scattering in bulk alloy semiconductors. (See publication numbers 14.)

(IV.4) SCATTERING DUE TO CLUSTERING EFFECTS IN III-V ALLOYS AND THEIR CONFINED STRUCTURES

Evidence for clustering in alloy semiconductors is often found, even though the degree of such clustering naturally depends upon the nature of the alloying species and the growth conditions. The clustering effect can be particularly important in influencing the transport and optical properties of confined carriers realized in heterojunctions, multiple quantum wells and superlattices involving an alloy layer, particularly when it is the well layer - for example in the  $\text{In}_{0.53}\text{Ga}_{0.47}\text{As}/\text{InP}$  system. Consequently we recently undertook an investigation of the role of clusters in influencing the low field, low temperature mobility of quasi 2-dimensionally confined electrons in isolated quantum wells. However, in the course of this investigation we recognized the inadequate nature of such investigations for bulk alloy systems themselves. It has become imperative that improvements be first made in the theory for bulk alloy semiconductors where the availability of data provides some testing ground for the reliability of the theory before it may be generalized to the confined carrier systems.

We have employed an extension of the proposal by Nordheim and Mott, (and subsequently employed by Harrison and Hauser for ternary III-V semiconductor alloys) to calculate the mobility for alloys with small degree of clustering. The cluster disorder potential is represented by a strength corresponding to the band edge discontinuity between the alloying compounds and a range corresponding to the average cluster size. The calculations are carried out within the Born approximation employed in earlier theories, as well as the more accurate phase shift analysis. Differences of about 10% in the

scattering cross section are found for the two cases. The mobility is studied as a function of the cluster size and for different alloy compositions.

Similar analysis is near completion for the  $In_xGa_{1-x}As/InP$  quantum well structures. In both, the bulk alloy and the 2D confined carrier systems, the presence of clustering is shown to reduce the mobility significantly, but its influence in the latter case is particularly damaging to the properties of the confined carriers. A manuscript on these calculations is presently under preparation. (See publication number 16.)

## V. ESTABLISHMENT OF TRANSPORT MEASUREMENT FACILITY

In anticipation of the growth of a variety of  $\text{GaAs}/\text{Al}_x\text{Ga}_{1-x}\text{As}$  based single and multiple interface structures in Molecular Beam Epitaxy laboratory at USC, we initiated the establishment of an electrical characterization and measurement facility. Such a facility was established, tested, and employed for measurements on some of the reasonable quality samples grown. This facility is capable of measuring d.c. conductivity and Hall mobility over the temperature range of  $4.2^\circ\text{K}$  to  $300^\circ\text{K}$ . Hall measurements in the Van der Pauw geometry can be carried out on samples of low as well as high impedance.

The cryogenics are based on a Janis (model #8DT) detachable tail type cryostat which affords considerable ease of operation. The insulation jacket is evacuated by a mechanical rotary pump to about  $10^{-3}$  Torr whence an ion pump (5 litres/sec) takes over to reduce the pressure to  $10^{-6}$  Torr. Cryoliquids are subsequently allowed into the dewar. Liquid helium temperature can be reached in the normal course. Although evacuation of the sample space can lower the temperature to about  $1.3^\circ\text{K}$ , this mode of operation is harder to achieve. The temperature controller is capable of covering the range  $4.2^\circ\text{K}$  to  $300^\circ\text{K}$  with an accuracy of  $0.1^\circ\text{K}$ . An electromagnet, a magnet power supply (up to 80 Amp) and a magnetometer circuit for measurement of magnetic fields up to 5 KG are included.

The system has been tested with a home-built (approximately 15 years ago) constant current supply capable of putting out currents between  $10^{-9}$  Amp to  $10^{-3}$  Amp, divided into three ranges, each having three selectable current values. A home-built electrometer-amplifier allows reliable measurements on low and high impedance samples in two modes of operation. These units were originally designed and built for measurements on bulk samples only. The requirements of the confined carrier in thin single and multiple interface structures, however, necessitated the need for modern digital current source

and electrometer with the capability of interfacing with a micro-computer. We have acquired such instruments and interfaced the complete system (with the exception of the magnet power supply) to an Apple IIe computer. The software has been developed and tested. We have employed the system for measurement of the Hall mobility on various MBE grown GaAs samples and have successfully reproduced reported results in the literature. We are presently adding on C-V and I-V measurements capability in both, pulsed (at 77°K) or steady state mode to separate out effects of interface states and lateral nonuniformities.

## REFERENCES

1. M. Voos, *Surf. Sci.* 113 94 (1982).
2. M. Horst, U. Merkt and J. P. Kotthaus, (to appear).
3. D. Olego, A. Pinczuk, A. C. Gossard and W. Wiegmann, *J. Vac. Sc. Tech. B* (April-June 1983, in press).
4. P. J. Price, *J. Vac. Sc. Tech.* 19, 599 (1981).
5. S. Mori and T. Ando, *J. Phys. Soc. Japan*, 48, 865 (1980).
6. J. Lee, H. N. Spector and V. K. Arora, *App. Phys. Letts.* 42, 363 (1983).

## PUBLICATIONS (Theory)

1. Electron-Phonon Interaction and Cyclotron Resonance in Two-Dimensional Electron Gas, B. Horowitz and A. Madhukar, *Solid State Comm.* 32, 695 (1979).
2. Electron-Phonon Coupling and Resonant Magneto-Phonon Effect in Optical Behaviour of Two-Dimensionally Confined Charge Carriers, A. Madhukar and S. Das Sarma, *Surf. Sci.* 98, 135 (1980).
3. Formation of an Anomalous Acoustic Plasmon in Spatially Separated Plasmas, S. Das Sarma and A. Madhukar, *Surf. Sci.* 98, 563 (1980).
4. Resonant Landau Level-Optical Phonon Interaction in Two-Dimensionally Confined Charge Carrier Systems, A. Madhukar, in *Theoretical Aspects and New Developments in Magneto-Optics*, Ed. J. T. Devresse, *NATO ASI Series B*, Vol. 60, p. 553 (1980).
5. Study of Electron-Phonon Interaction and Magneto-Optical Anomalies in Two-Dimensionally Confined Systems, S. Das Sarma and A. Madhukar, *Phys. Rev. B22*, 2823 (1980).
6. Self-Consistent Theory of Screening in a Two-Dimensional Electron Gas Under Strong Magnetic Field, S. Das Sarma, *Solid State Comm.* 35, 357 (1980).
7. Collective Modes of Spatially Separated, Two-Component, Two-Dimensional Plasma in solids, S. Das Sarma and A. Madhukar, *Phys. Rev. B23*, 805 (1981).
8. Theory of the Transverse Static Magnetoconductivity in a Two-Dimensional Electron-Phonon System, M. Grabowski and A. Madhukar, *Solid State Comm.* 41, 29 (1982).
9. Quantum Theory of Magnetotransport in Two Dimensional Systems with Electron-Impurity, Electron-Phonon and Electron-Electron

Interactions, M. Grabowski and A. Madhukar, *Surf. Sci.* 113, 273 (1982).

10. A Theory of Cyclotron Resonance in a Two-Dimensional Quantum Wigner Crystal, B. Horowitz, M. Grabowski and A. Madhukar, *Surf. Sci.* 113, 318 (1982).
11. Energy levels of n-channel Accumulation Layer on InP Surface, S. Das Sarma, *Solid State Comm.* 41, 483 (1982).
12. Metastable and Modulated Structures: Prospects for Future Studies, F. J. Grunthaner and A. Madhukar, *J. Vac. Sc. Tech.* B1, 462 (1983).
13. Quantum Size Effect in the Transport of electrons in Semiconductor Quantum Well Structures, S. B. Ogale and A. Madhukar, *App. Phys. Letts.* (submitted)
14. Alloy Disorder Scattering Contributions to Electron Mobility in Semiconductor Quantum Well Structures, S. B. Ogale and A. Madhukar, *J. App. Phys.* (submitted)
15. Theory of the Remote Ion, Interface Roughness and Alloy Disorder Scattering Contributions to the Low Temperature Electron Mobility in Thin Quantum Well Structures, S. B. Ogale and A. Madhukar, *Phys. Rev. B* (to be submitted).
16. Effect of Alloy Clustering on Carrier Transport in III-V Compound Semiconductors and Their Confined Structures, J. Singh, S. B. Ogale and A. Madhukar, (In preparation).

## PERSONNEL: (Theory)

1. Anupam Madhukar, Co-P.I. (1977-1983)
2. B. Horowitz, Post Doctoral Visitor (1978-1979)
3. S. Das Sarma, Post Doctoral Visitor (1979-1980)
4. M. Grabowski, Post Doctoral Visitor (1980-1981)
5. S. B. Ogale, Post Doctoral Visitor (1982-1983)
6. Andre Fedotowsky, Post Doctoral Visitor (1982-1983)
7. William Post, Graduate Student (1978-1979; 1982)
8. J. Y. Kim, Graduate Student (1981-1983).

Final Report

Experimental Studies of the Magneto-Transport  
and Magneto-optical characteristics  
of two-dimensional heterostructures

Air Force Office of Scientific Research  
Contract AFOSR 78-3530A

Funding period 7 December 1978  
through 31 March 1983



Submitted by N.P. Ong  
Associate Professor of Physics  
University of Southern California  
Los Angeles, CA 90089-0484  
Date 7/10/83

CONTENTS

A. Introduction and background.....	1
B. Molecular Laser Spectrometer.....	4
C. Results on HgTe/CdTe superlattice.....	5
1. Galvanomagnetic studies.....	5
2. Photoconducting studies.....	8
D. (TMTSF) <sub>2</sub> PF <sub>6</sub> salt.....	8
E. References.....	11
F. Table 1.(Far-infrared laser lines.).....	14
G. Figure Captions.....	15
H. Figures 1-9.....	18

Final Report on Air Force Office of Scientific Research

Contract AFOSR 78-3530A

Period 7-Dec-78 through 31-Mar-83.

A. Introduction and background.

Objective. The goals of this project were 1) to set up a far-infrared (FIR) laser spectrometer system to study the low-temperature and high magnetic field electronic properties of semiconductor systems in quasi-two-dimensional structures, and 2) to perform dc galvanomagnetic studies of these systems to augment the studies in 1.). The overall emphasis of this project as originally conceived was to concentrate on systems based on the III-V compounds such as GaAs, GaAlAs and InP.

Accomplishments. A molecular gas laser pumped by a CO<sub>2</sub> laser was constructed and upgraded over the period of the contract. The final version produces FIR laser lines in the spectral range 11 cm<sup>-1</sup> through 120 cm<sup>-1</sup>. The frequency coverage (12 lines) is good enough for spectroscopic studies of broad absorptions lines in this difficult part of the electromagnetic spectrum. Power levels ranged from 100 microwatts to one milliwatt depending on the line. The spectrometer was used to study two novel low-dimensional

synthetic metals which show promise for detector applications in this frequency range. These are 1.) superlattices made of alternating layers of HgTe and CdTe, and 2) the organic synthetic metal bis-tetramethyltetraselenafulvalene hexafluorophosphate,  $(TMTSF)_2 PF_6$ . Photoconducting responses at wavelengths peaked near  $20\text{ cm}^{-1}$  were found in these two compounds. (See below.) In support of the submillimeter work we also performed extensive galvanomagnetic work on the HgTe/CdTe superlattice as well as on Si-MOSFET devices at high fields (up to 19 Teslas) and at low temperatures (down to 0.5 Kelvin.) No galvanomagnetic work was performed on the TMTSF salt since rather complete reports exist in the recent literature.

Sample source problems. The major difficulty we faced during this project was the acquisition of good quality samples of heterostructures or MISFETs (metal-insulator-semiconductor field effect transistors) made from III-V semiconductors. We obtained several Si-MOS (metal-oxide-semiconductor) capacitors (which are of less relevance to the project goals) from Robert Wagner of the Naval Research Research Lab., Arlington. However, efforts to obtain MISFETs based on InP from Hughes Lab., Malibu were ultimately unsuccessful. We had also hoped to acquire heterostructures of GaAs/GaAlAs from the molecular-beam-epitaxial machine recently set up at the

University of Southern California (USC), but unexpected difficulties with this machine forced us to look at outside sources.

New Sample Sources. These difficulties have been overcome and we now have reliable access to several groups at Rockwell International Science Center, Thousand Oaks, who have supplied us with high mobility samples. The HgTe/CdTe samples to be discussed below are made by a novel laser flash technique by Dr. Jeff Cheung at Rockwell. The fabrication of novel superlattice structures based on other combinations of matched semiconductors is possible using this technique. The organic metals were grown by Dr. Ed Engler of IBM, San Jose. Professor Dan Dapkus (Materials Science, USC) has also agreed to supply high mobility InP/InGaAs heterostructures grown by MOCVD. Dr. S. J. Lee of USC and Rockwell, Thousand Oaks has recently designed high speed circuits based on GaAs/GaAlAs MISFETs. He has given us some of these transistors for low-temperature work. Unfortunately, these sources appeared too late to impact on the present project. The rest of the report will be confined to discussions on the molecular laser system, and results obtained on HgTe/CdTe superlattice and the TMTSF salt.

### B. Molecular Laser Spectrometer.

In our set-up a  $\text{CO}_2$  cw laser (30 watts output) is used to pump a molecular gas laser<sup>1</sup> (Figure 1.) Depending on the gas used the laser lines in the far-infrared (FIR) deliver 100 microwatts to 1 milliwatt and span the spectral region  $11 \text{ cm}^{-1}$  through  $120 \text{ cm}^{-1}$ . By using only four non-toxic gases<sup>2</sup> we attain reasonable coverage of this region (Table 1.) The lower limit is still short of the reach of conventional millimeter microwave sources ( $90 \text{ GHz} \approx 3 \text{ cm}^{-1}$ ,  $1 \text{ cm}^{-1} \approx 1.5\text{K}$ ) The upper limit is imposed by our optics. Polyethylene lenses are used for the FIR part of the optics. One-inch copper pipes are used as oversized waveguides to direct the FIR beam into the bore of a superconducting magnet (10 Tesla maximum.) FIR detection at room temperature is by a pyroelectric detector. At liquid He temperatures a carbon bolometer is used to measure transmission through the sample. Typically the pump beam is chopped at 13 Hz and the bolometer temperature modulation at this frequency is detected by lock-in amplifiers. In the photoconducting studies discussed below the resistance of the sample is monitored using a bridge and resistance modulation at 13 Hz detected by lock-in amplifiers. For experiments requiring magnetic field sweep the FIR laser output has been stabilised to 1 % for about 1 hour. A report on the experimental apparatus will be submitted to

Review of Scientific Instruments.

C. Results on HgTe/CdTe superlattice.

The bulk alloy  $Hg_{1-x}Cd_xTe$  has been the source of great interest<sup>3</sup> because its gap can be varied from zero through 1.6 electron volts as  $x$  varies from 0 to 1. Efforts to optimise the efficiency of the bulk alloy in FIR detection have been complicated by stoichiometric problems, inhomogeneous gap variation, and alloy stability. Recently it was suggested by Schulman and McGill<sup>4</sup> that some of these difficulties may be avoided by forming a superlattice of alternating layers of pure HgTe and CdTe. They calculated that the gap can be varied by tuning the layer thickness rather than changing the alloy composition. In July 1982 Dr. Cheung<sup>5</sup> at Rockwell succeeded in growing good quality superlattices by a laser flash evaporation technique and made the first samples available to us (Figure 2.) Rather extensive galvanomagnetic and FIR absorption measurements have been performed on these samples and are being submitted for publication<sup>6-9</sup>. Some measurements were made at the National Magnet Lab., Cambridge. The main results are as follows.

1.) Galvanomagnetic studies. Because of the quasi-two-dimensional (2d) confinement of the electron gas in the HgTe layer the conducting properties of the

electrons are dominated by two-dimensional effects which have been actively studied by physicists in the last four years. Following a seminal paper by Thouless<sup>10</sup> on the behavior of one-dimensional disordered metals at low temperatures, Abrahams et al<sup>11</sup> proposed a single parameter scaling model (Figure 3) which predicted that no truly two-dimensional metal can exist. (As the temperature T decreases the resistivity should diverge as  $\log T$  regardless of the purity of the 2d system.) This model is now known as weak or incipient localisation. Shortly thereafter Altshuler et al<sup>12</sup> predicted the same logarithmic divergent behavior for 2d systems, but based on an entirely different effect. In this competing theory the logarithmic divergence is caused by Coulomb interaction between the electrons (Interaction theory.) The logarithmic behavior<sup>13</sup> has now been observed in Si-MOSFETs<sup>14</sup>, quenched metal alloy films<sup>15</sup>, GaAs/GaAlAs heterostructures, InO films<sup>16</sup>, Pt films<sup>17</sup> and copper films<sup>18</sup>. In HgTe/CdTe superlattice we observed<sup>6</sup> the logarithmic rise of the dc resistance starting at relatively high temperatures (30K) and extending down to 0.5K (Figure 4.) Most studies show that the logarithmic increase is due to a combination of the two effects (localisation and Coulomb interaction.)

In HgTe/CdTe the Coulomb interaction effect appears to dominate the incipient localisation effect.

Magnetoresistance and Hall measurements are effective tools

for distinguishing the two effects. We have performed such studies at fields up to 19 Teslas and T down to 0.5 K and find that the Coulomb correlation effect is quite large in this novel system. A rapid communication<sup>6</sup> in Physical Review on this work is in press.

A novel phenomenon predicted by Lee and Ramakrishnan<sup>19</sup> (and first seen in Si-MOSFETs<sup>20</sup>) involves the Zeeman splitting of the spin degeneracy. This suppresses one of the Feynmann diagrams which lead to a logarithmic decrease of the resistance. The net result is a positive longitudinal magnetoresistance (field parallel to sample) which is logarithmic. A striking confirmation of this spin-dependent magnetoresistance was obtained by us in HgTe/CdTe<sup>7</sup> and will be submitted for publication shortly (Figure 5.) One of the tests commonly used to disentangle the relative contributions of the two effects (localisation and Coulomb interaction) to the observed logarithmic rise in the sample resistance is the Hall effect. Localisation theory predicts no change in the Hall voltage whereas a logarithmic increase (with decreasing T) is expected in the Interaction theory. In Fig. 6 we show the temperature dependence of the low field Hall constant. It is clear that interaction effects are playing a dominant role in this system. Shubnikov-de Haas oscillations at high fields (above 6 T) were also seen in the Hall voltage and transverse magnetoresistance, (Fig. 7) although the quantum

oscillations are not as pronounced as in the GaAs/GaAlAs systems. A paper<sup>8</sup> on this work is also in preparation.

2. Photoconducting studies. Photoconduction studies were performed on the HgTe/CdTe superlattices at the FIR wavelengths indicated in Table 1. We observed<sup>9</sup> a strong absorption peak (corresponding to a rise in conduction) at  $20 \text{ cm}^{-1}$  (Figure 8, upper panel.) This corresponds to a localised resonant state approximately 2 mev above the Fermi level in the conduction band of the HgTe. Although a similar feature has already been observed in bulk HgTe and ascribed to vacancies in the Te, our observation in a 2d realisation of HgTe may force some re-interpretation of the absorption peak. To verify that the absorption line is electronic in origin we applied magnetic fields of 0.6 and 6 Teslas and found that the absorption line moves to lower frequencies and is eventually suppressed (Fig. 8, lower panel.) This is consistent with the motion of the lowest Landau level through the localised state. A publication on this observation is in preparation<sup>9</sup>.

(TMTSF)<sub>x</sub>PF<sub>6</sub> salt.

The discovery of superconductivity in organic metals<sup>21</sup> in the family of salts made from TMTSF and its close derivatives has caused great excitement in Solid State Physics and Chemistry<sup>22</sup>. The PF<sub>6</sub> compound was the first to

show superconductivity ( at 1 Kelvin and under 12 kbar pressure.) At ambient pressure no superconductivity is observed. Instead, a spin-density-wave (SDW)<sup>23</sup> state appears at 12K. The resistance becomes activated<sup>24</sup> below this temperature because of the SDW gap formed over the full Fermi surface. Although the Arrhenius plot of the resistivity showed the presence of a gap of 24K no optical evidence of this gap exists in the literature because of the difficulty of performing FIR studies at this low frequency using Fourier transform methods.

Our FIR laser spectrometer has certain advantages over techniques based on classical sources because of the high powers available. Our motivation for taking up this study was two-fold. First, direct spectroscopic evidence for the SDW gap is more reliable than transport evidence. For example, one can directly monitor the gap variation with magnetic field. (This is difficult with dc resistivity because of the strong mobility dependence on field.) Secondly, non-bolometric detectors in this spectral region are few in number because well defined gaps of this magnitude are difficult to realise in solids. The presence of localised states in the density of states of narrow-gap semiconductors, for example, tend to obscure such gaps. The advantage of using gaps arising from electronically driven instabilities (such as charge density wave or spin density wave states) is that such gaps are sharp and have values

ranging from 5K through 400 K. A good photoconductor in this frequency band would find wide applications. Our results<sup>25</sup> show that the PF<sub>6</sub> salt can indeed be used as a sensitive photoconductive detector for frequencies exceeding 20 cm<sup>-1</sup> (twice the gap value.)

Figure 9 shows the change in conductance versus the incident laser frequency in the range 11 cm<sup>-1</sup> through 100 cm<sup>-1</sup>. Below 20 cm<sup>-1</sup> no photoabsorption is observed, consistent with a gap value of 16 K. This is consistent with the dc resistivity data on the same sample. A major problem in working with this material is its fragility. Unless the sample is cooled slowly in a strain free environment it cleaves in one of its easy planes. We intend to study other derivatives of this salt to search for other photodetectors. This study<sup>25</sup> is still in progress.

References.

1. T. Y. Chang and T. J. Bridges, *Optics Commun.* 1, 423, (1970).
2. See for e.g. B. L. Bean, and S. Perkowitz, *Optics Lett.* 1, 202 (1977).
3. For a review see R. Dornhaus, G. Nimtz, and W. Richter, *Springer Tracts Mod. Phys.* 78(1976).
4. J. N. Schulman and T. C. McGill, *Appl. Phys. Lett.* 34(10), 663 (1979).
5. J. T. Cheung and D. T. Cheung, *J. Vac. Sci. Tech.*, 21, 182 (1982); J. T. Cheung, M. Khoshnevisan, and T. McGee, *Appl. Phys. Lett.*, submitted.
6. N. P. Ong, G. Kote, and J. T. Cheung, *Phys. Rev.* 827, Aug. 15, 1983.
7. N. P. Ong, G. Kote, J. T. Cheung, and P. Tedrow, unpublished.
8. G. Kote, N. P. Ong, and J. T. Cheung, unpublished.
9. F. Scero, N. P. Ong, and J. T. Cheung, unpublished.
10. D. J. Thouless, *Phys. Rev. Lett.* 32, 1167 (1977).
11. E. Abrahams, P. W. Anderson, D. C. Licciardello,

and T. V. Ramakrishnan, Phys. Rev. Lett. 42, 673 (1979).

12. B. L. Altshuler, A. G. Aronov, and P. A. Lee, Phys. Rev. Lett. 44, 1288, (1980); B. L. Altshuler, D. Khmel'nitskii, A. I. Larkin, and P. A. Lee, Phys. Rev. B22, 5142 (1980).

13. For a review see Proceedings of the Fourth International Conference on Electronic Properties of Two-Dimensional Systems, New London, 1981.

14. D. J. Bishop, D. C. Tsui, and R. C. Dynes, Phys. Rev. Lett. 46, 360 (1981).

15. G. J. Dolan, and D. D. Osheroff, Phys. Rev. Lett. 43, 721 (1979).

16. Zvi Ovadyahu, and Yoseph Imry, Phys. Rev. B24, 7439 (1981).

17. R. S. Markiewicz and L. A. Harris, Phys. Rev. Lett. 46, 1149 (1981).

18. Dov Abraham, and Ralph Rosenbaum, Phys. Rev. B27, 1409 (1983); ibid. B22, 1413 (1983).

19. P. A. Lee and T. V. Ramakrishnan, Phys. Rev. B26, 4009 (1982).

20. D. J. Bishop, R. C. Dynes, and D. C. Tsui, Phys. Rev. B25, 773 (1982).

21. D. Jerome, A. Mazaud, M. Ribault, and K. Bechgaard, J. Physique Lett. 41, L-95, (1980); D. Jerome, J. Phys. Soc. Japan 49 Suppl. A 845 (1980).
22. See for example, Proceedings of the International Conference on Low-Dimensional Conductors, Boulder, 1981. in Mol. Cryst. and Liq. Cryst., 22, 1-356 (1981).
23. W. M. Walsh, F. Wudl, G. A. Thomas, D. Nalewajek, J. J. Hauser, P. A. Lee, and T. Poehler, Phys. Rev. Lett. 45, 829 (1980).
24. P. M. Chaikin, G. Gruner, E. M. Engler, and R. L. Greene, Phys. Rev. Lett. 45, 1874 (1980).
25. F. Soero, N. P. Ong, and E. M. Engler, unpublished.

• Table 1.

Far-infrared laser lines.

Table shows the lasing medium and the typical power obtained.

GAS	WAVELENGTH	FREQUENCY	POWER
$\text{CH}_3\text{OH}$	70 micron	$143 \text{ cm}^{-1}$	0.1-0.2 mw
$\text{CH}_3\text{OH}$	96	104	0.1-0.2
$\text{CH}_3\text{OH}$	118	85	1.0
$\text{CH}_3\text{OH}$	163	61	0.1
$\text{CD}_3\text{OD}$	184	54	0.1-0.2
$\text{CD}_3\text{OD}$	255	39	0.1-0.2
$\text{HCOOH}$	393	25	0.6
$\text{HCOOH}$	432	23	0.6
$\text{HCOOH}$	513	19	0.5
$\text{CH}_3\text{OH}$	578	17	0.1-0.2
$\text{CH}_2\text{CF}_2$	663	15	0.1-0.2
$\text{CH}_2\text{CF}_2$	890	11	0.3

Figure Captions

Figure 1. Schematic drawing of the far-infrared laser and the  $\text{CO}_2$  pump laser.

Figure 2. Electron microscope photograph of an etched pit in a sample of  $\text{HgTe}/\text{CdTe}$  superlattice. The individual layers of  $\text{HgTe}$  are 110 angstroms thick; the  $\text{CdTe}$  layers are 220 angstroms thick. 155 layers are laid down on a  $\text{CdTe}/\text{GaAs}$  substrate (Ref. 5.)

Figure 3. The scaling diagram of sample conductance versus the size  $L$  of the sample for disordered conductors. The x-axis shows the log of the conductance  $g$ ; the y-axis  $\beta$  is the derivative of log  $g$  with respect to log  $L$ . The three flow trajectories are for samples of 1, 2 and 3 dimensions. Good conductors are on the right of the graph; good insulators are on the left. The log  $T$  behavior in 2d systems traces the middle trajectory as  $T$  decreases. (From Ref. 11.)

Figure 4. The resistance per square of  $\text{HgTe}/\text{CdTe}$  superlattice versus log  $T$  at zero field (Sample 1). The bottom inset shows the log behavior down to 0.5K for a Sample 2. The top inset shows the full temperature dependence up to 300K (Ref. 6.)

Figure 5. The longitudinal magnetoresistance of

HgTe/CdTe superlattice at various temperatures. Below 2 Teslas the resistance rises logarithmically with field in agreement with the theory of Lee and Ramakrishnan<sup>19</sup>. Because the field is parallel to the current ( $I$ ) here and the same behavior is also observed with field perpendicular to  $I$  (but still in the plane) we associate this magnetoresistance with the Zeeman splitting of the electronic spin. The resistance above 2 Teslas is due to a spin-dependent quadratic background which may be a bulk effect. (Ref. 7.)

Figure 6. The temperature dependence of the low-field Hall constant in HgTe/CdTe superlattice (Sample 1.)  $N_1$  is the number of active layers (Ref. 6.)

Figure 7. The transverse magnetoresistance of HgTe/CdTe superlattice at low temperatures and high fields. Measurements were taken with an ac current (1 kHz.) The curves above the x-axis are the in-phase (resistive) voltage signal across the sample for temperatures between 0.5 and 2 K. The region above 14 Teslas is strongly temperature dependent and may be evidence for a quantum state quite different from a normal electron gas. The curves below the x-axis are the out-of-phase (reactive) component of the voltage. Note the strong dispersion seen when the field exceeds 14 Tesla (Ref. 6.)

Figure 8. The photoconducting response of HgTe/CdTe

superlattice versus frequency in the FIR region. In the upper panel (field zero) the absorption peaks at  $26\text{ cm}^{-1}$  (2.5 mev). The resonant state is identified with a localised state resonant with the conduction band and 2.5 mev above the Fermi level. When a magnetic field is applied (lower panel) the absorption line is broadened towards low frequencies at 0.6T and is eventually totally suppressed at 6 Teslas. This behavior is consistent with an electronic origin for the absorption. A strong field causes the lowest Landau level to move towards the resonant state (Ref. 9.)

Figure 9. Photoconductance response of a single crystal of  $(\text{TMTSF})_2\text{PF}_6$  versus frequency in the FIR region. The gap associated with the spin-density-wave state which appears at 12 K was found to be 16K by dc resistance measurements in this sample. In the optical absorption data here one sees photoconductive response starting at  $22\text{ cm}^{-1}$  which corresponds to twice the SDW gap. (unpublished.)

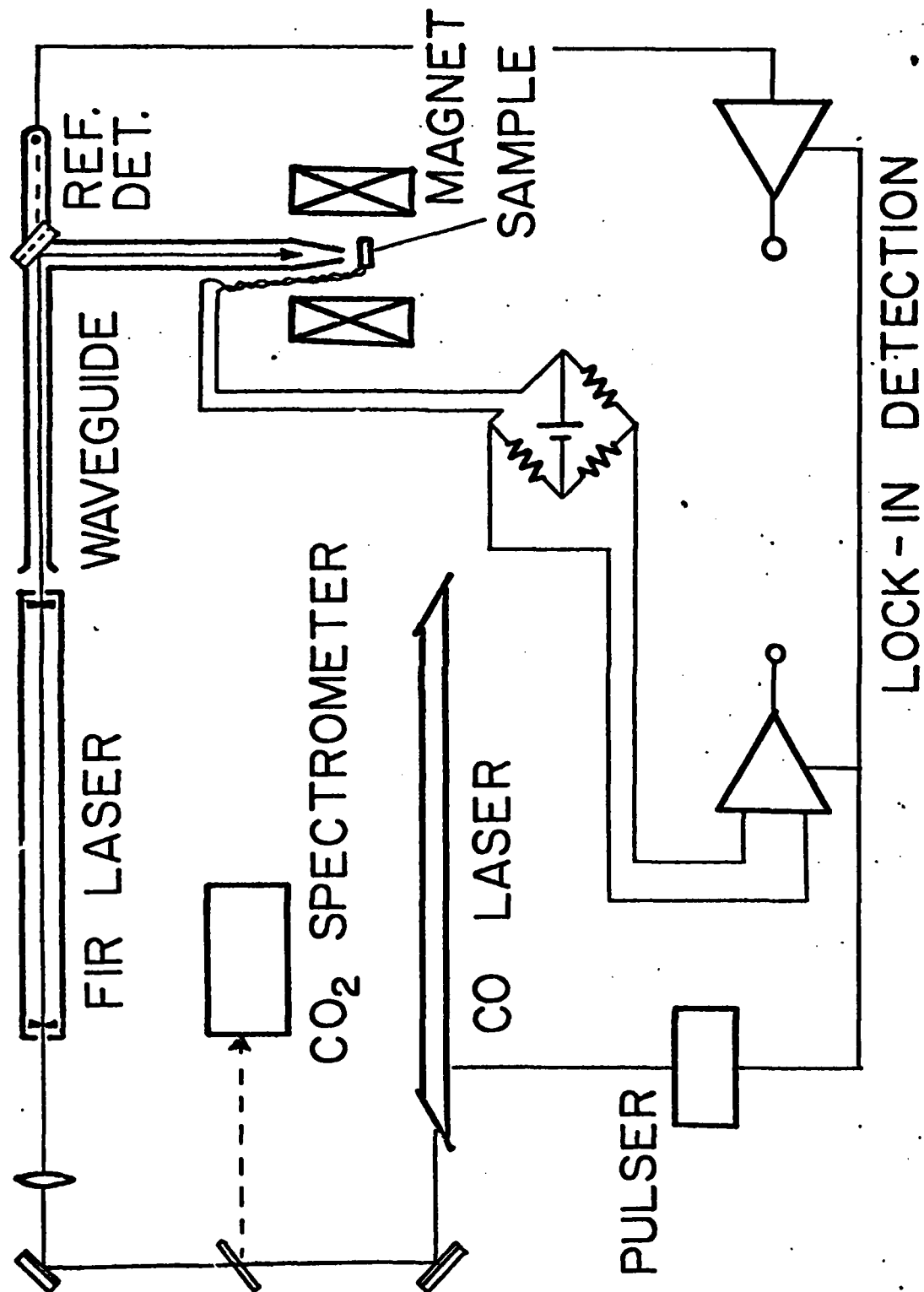


Figure 1

# LADA GROWN HgTe/CdTe SUPERLATTICE

SC82-19349

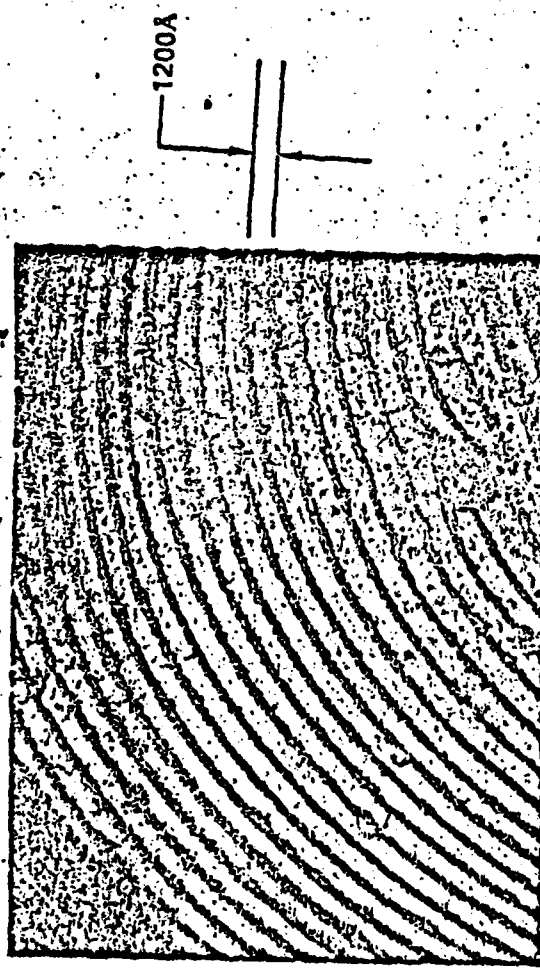


Figure 2

CROSS SECTION OF AN ANGLE-ETCHED SAMPLE



Rockwell International  
Science Center

FIG. 2

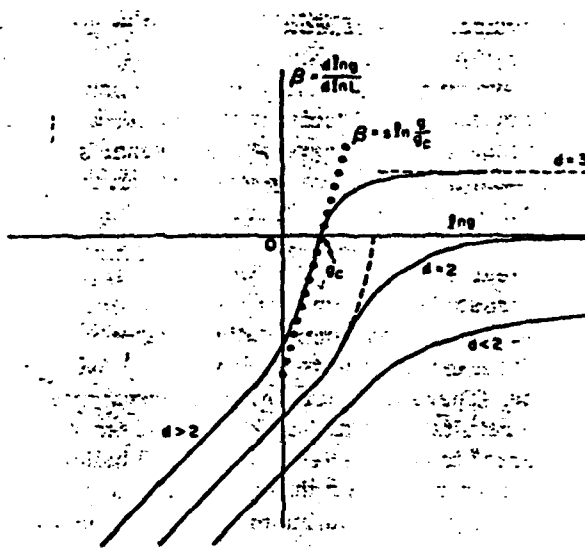


FIG. 3. Plot of  $\beta(g)$  vs  $\ln(g)$  for  $d > 2$ ,  $d = 2$ ,  $d < 2$ .  $g(L)$  is the normalized "local conductance." The approximation  $\beta = s \ln(g/g_c)$  is shown for  $g > 2$  as the solid-circled line; this unphysical behavior necessary for a conductance jump in  $d = 2$  is shown dashed.

Figure 3

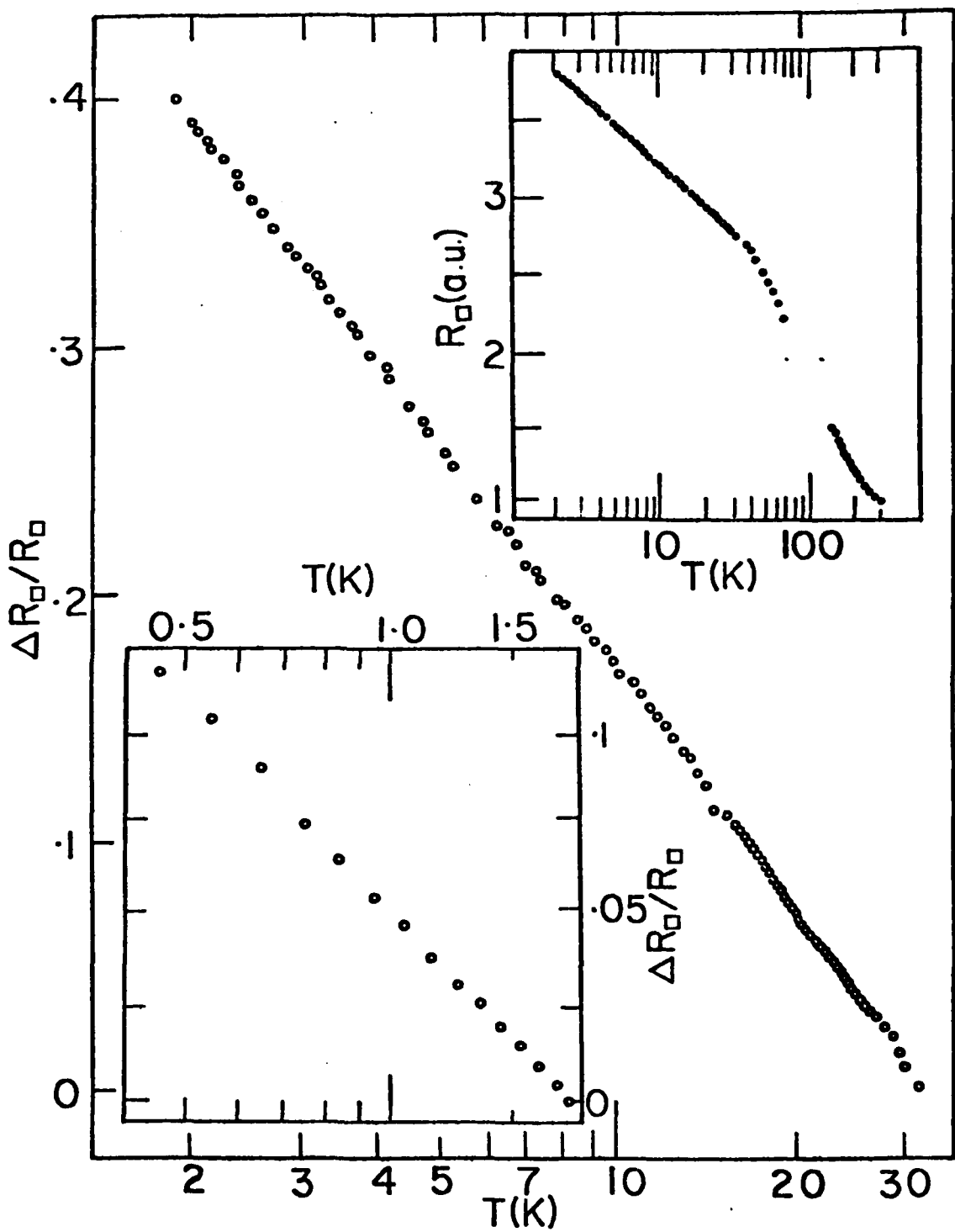


Figure 4

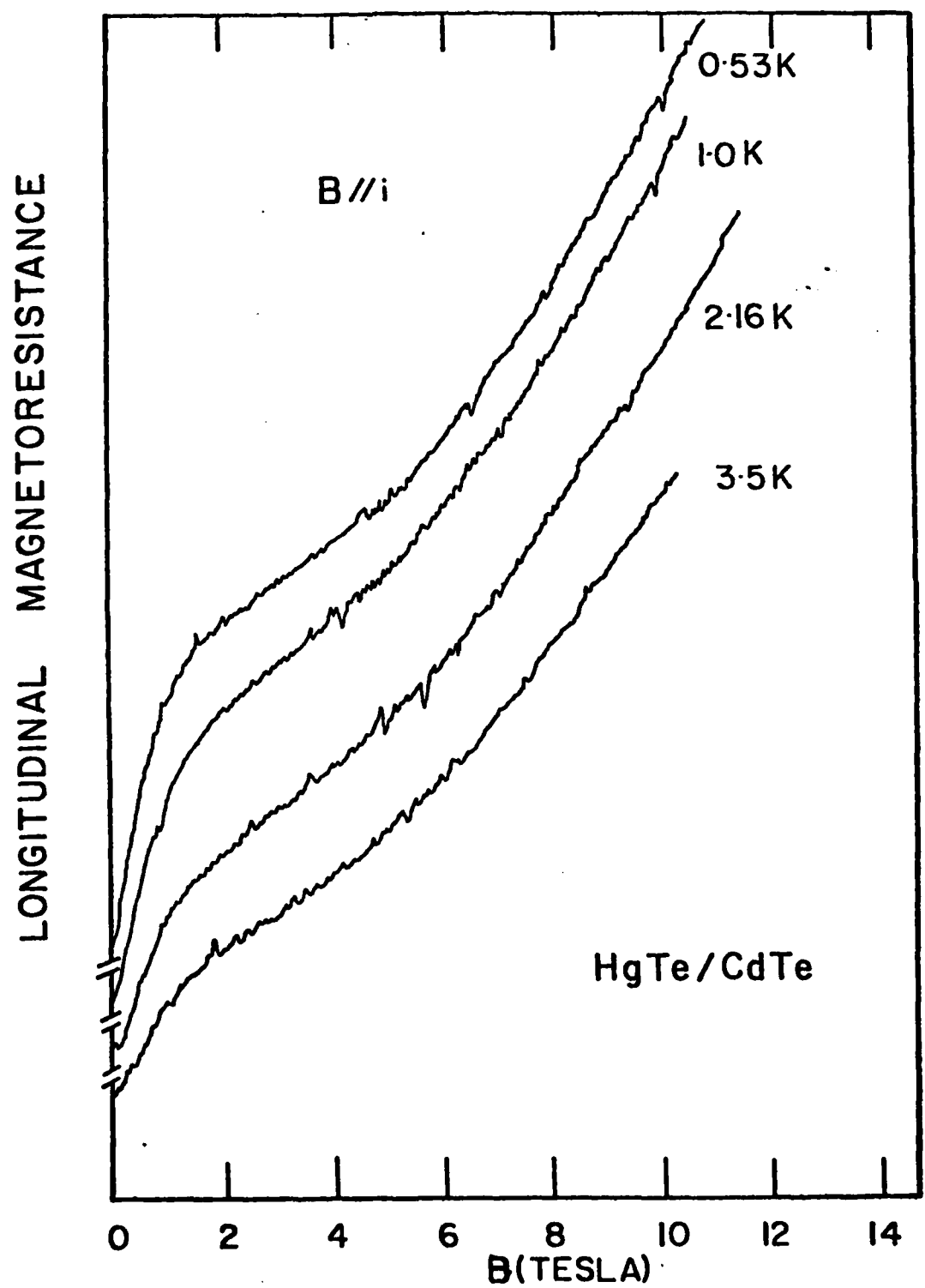


Figure 5

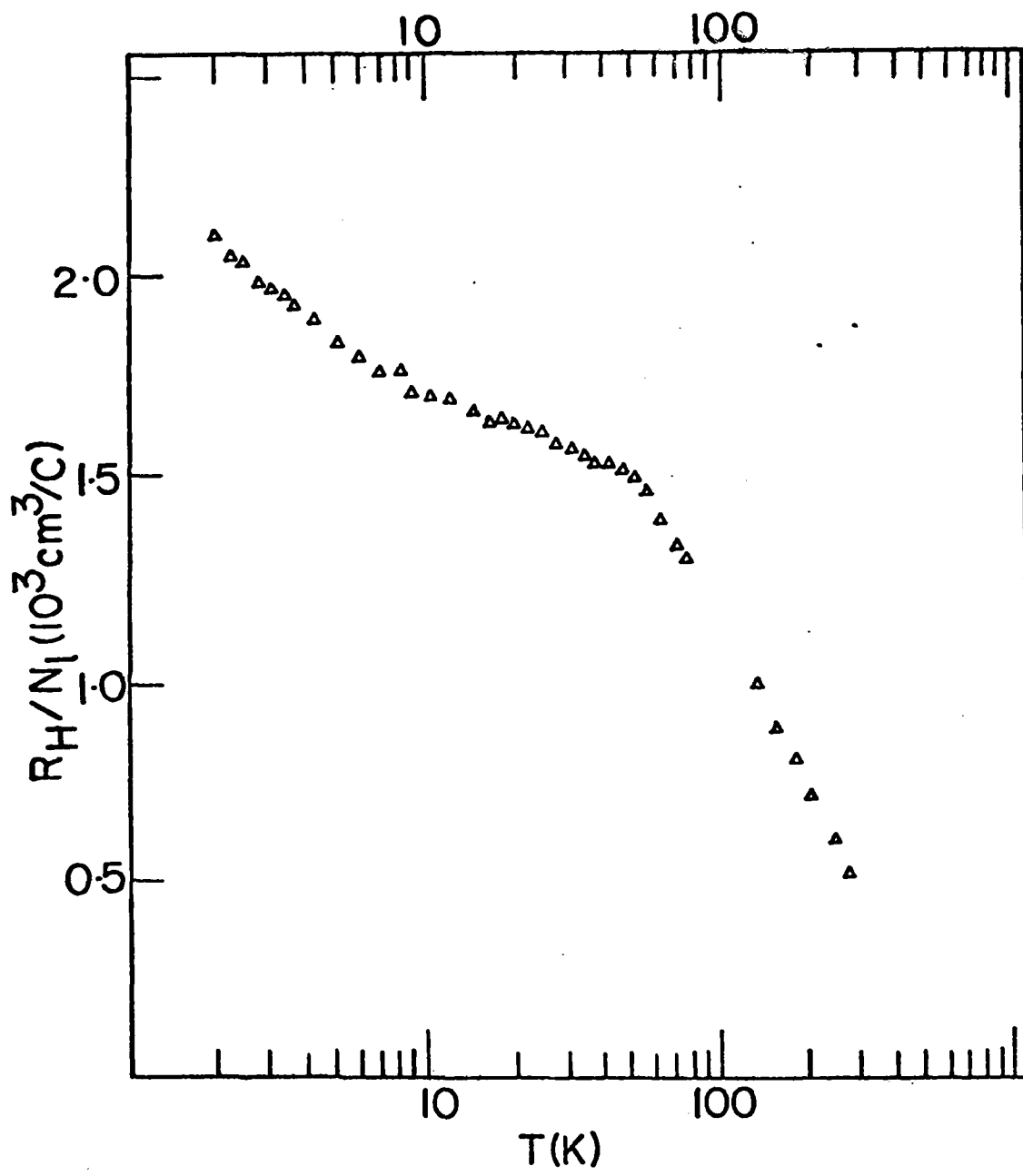


Figure 6

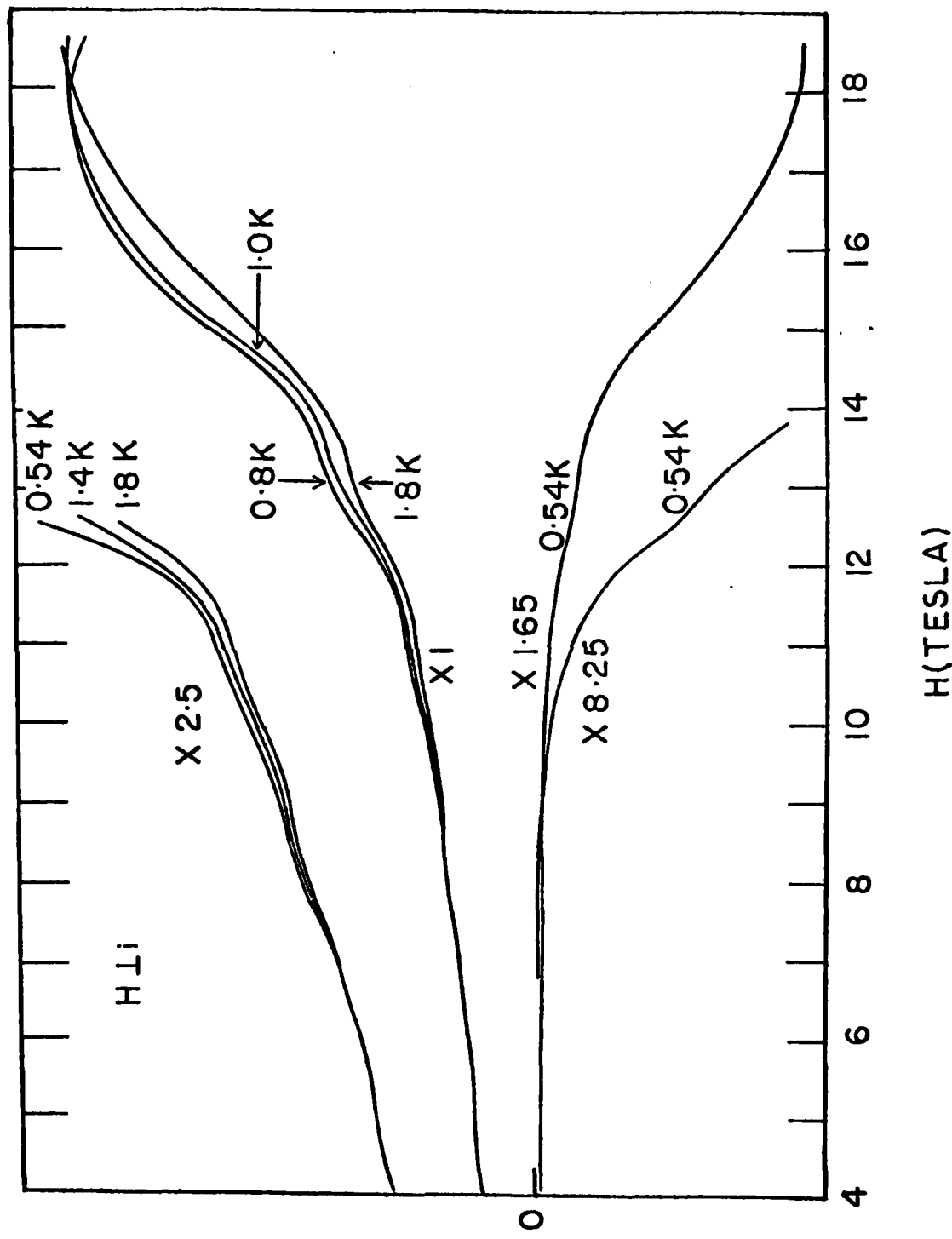


Figure 7

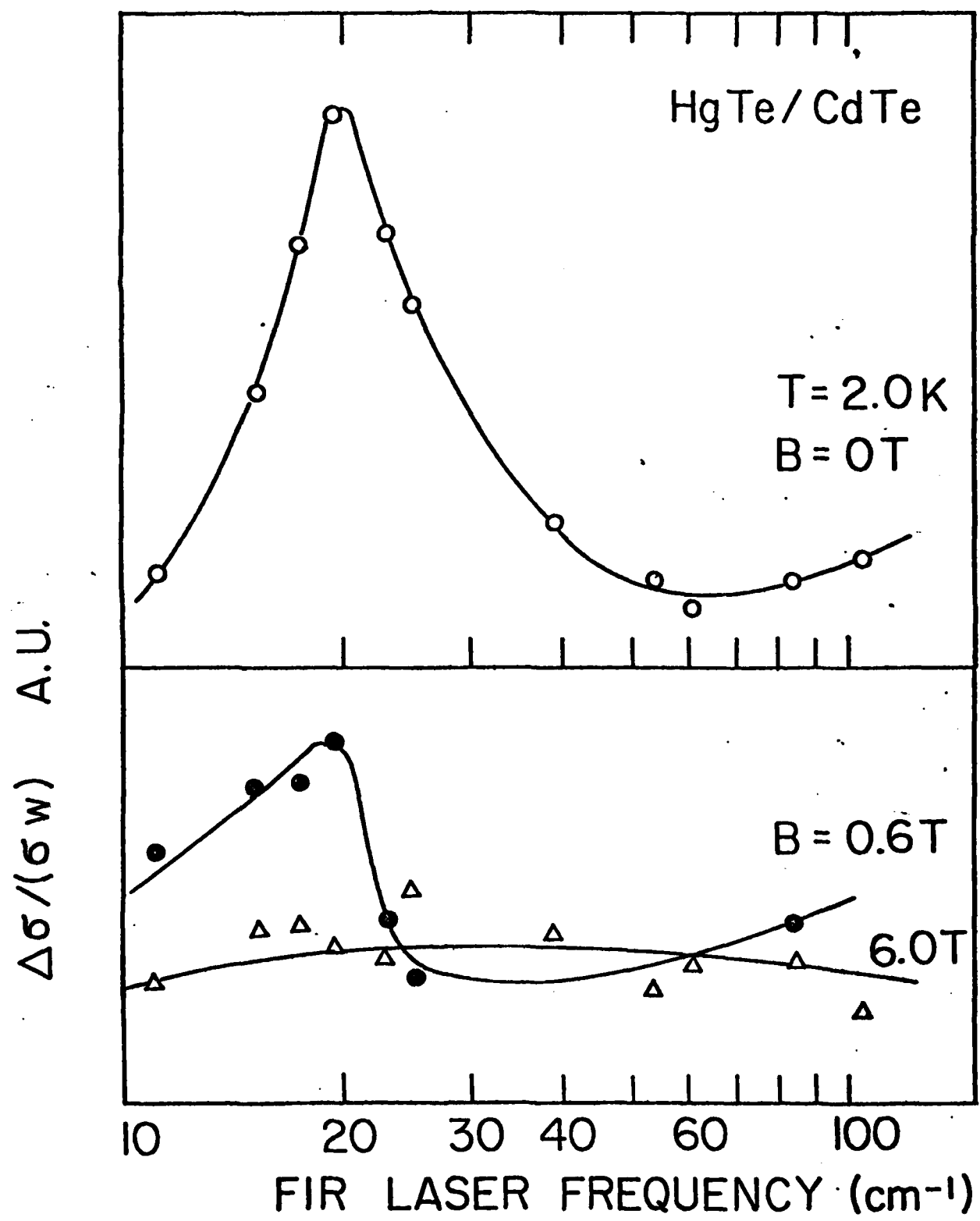


Figure 8

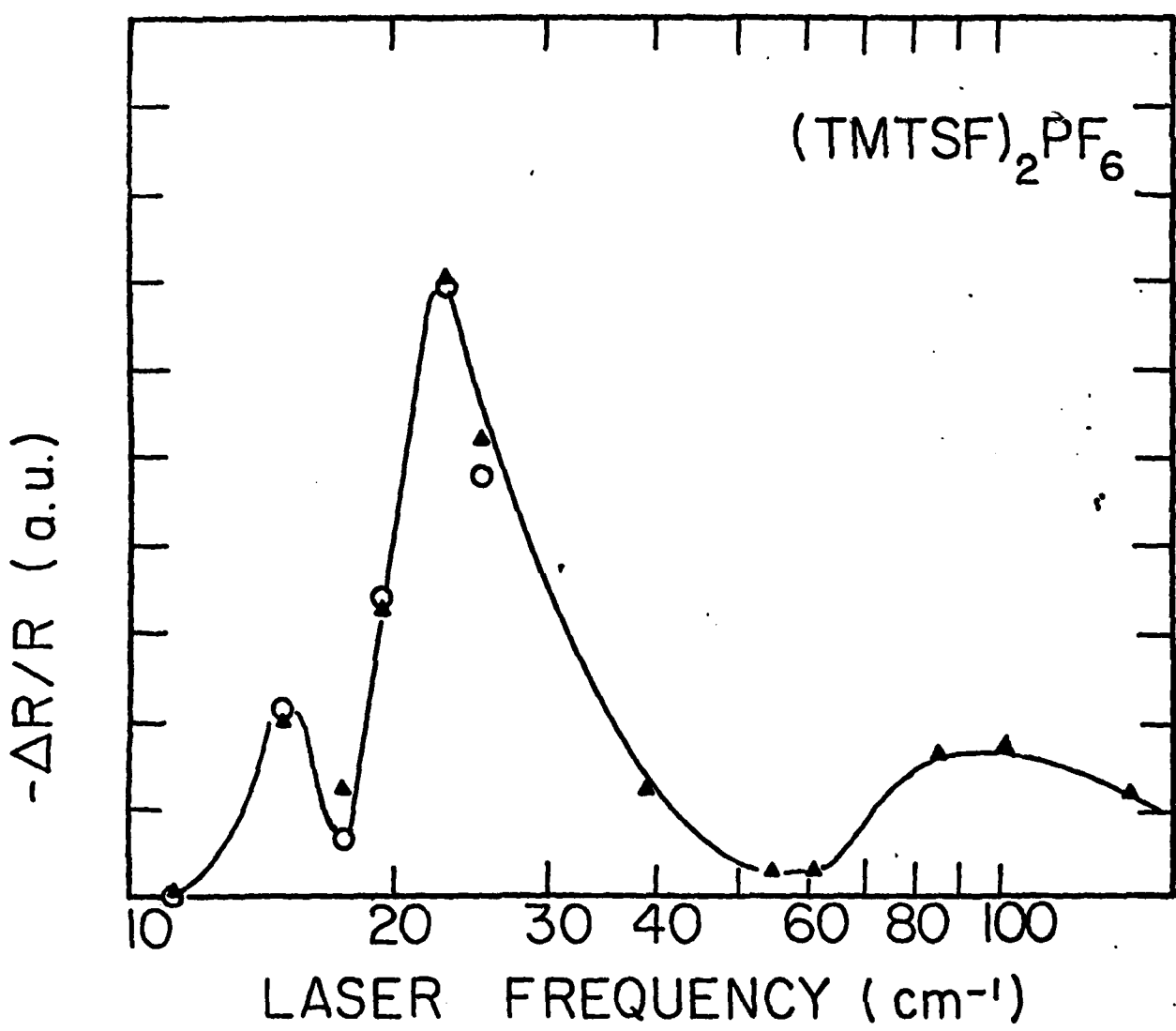


Figure 9